STRANGE PARTICLE SIGNATURES OF THE HADRONIC MATTER DECONFINEMENT PHASE TRANSITION[1]

Johann Rafelski

Department of Physics
University of Arizona, TUCSON AZ 85721

ABSTRACT: Relativistic nuclear collisions offer a unique opportunity to study hot hadronic matter and to discover the quark gluon plasma. The large scales of the colliding nuclei increase the likelihood of generating highest energy densities for longest available times. Current results suggest that even at 200 A GeV one needs hardly more than the diameter of a heavy nucleus, 15 fermi, to stop a ^{32}S-projectile. Strange particle yields are suggestive of new reaction mechanisms and prove to be a most useful diagnostic tool in the study of nuclear matter under extreme conditions.

OVERVIEW

The critical question posed by relativistic heavy ion experiments is that of deconfinement and quark gluon plasma (QGP) formation: I am eagerly awaiting first results on multi-strange antibaryons, which I consider most informative observables of the deconfined QGP phase. Multi-strange antibaryons can provide this crucial information as they are formed predominantly in phase space regions in which a very high strangeness density is present since they are produced almost totally by glue-glue processes in the QGP. The over-abundance of multistrange antibaryons stemming from QGP formation could, in theory, be reduced in a scenario where the antibaryons would be kept together for an anomalously long time, during which re- equilibration of strangeness would occur. However, the effects of such a long lifetime of the hadronic phase should then also be discernible in other strange and non-strange observables. Furthermore, we can focus our "cameras" on early times in the reaction by looking at multi-strange antibaryons at moderately high transverse momenta above 1 GeV which are more representative of the bare particle abundances in the high energy density initial fireball, as hadronization mechanisms do not populate this 'hard' region abundantly. Aside from its most important role as a characteristic observable of the deconfinement phase transition, observation of strange particle flows provides information about the reaction mechanisms governing relativistic nuclear collisions: for example the Λ abundance traces out the flow of baryon number. In general, the large strangeness production

[1]From: *Hadronic Matter in Collision 1988*, pages 776–790 (World Scientific 1989), ISBN 9971-50-849-4, P. Carruthers, J. Rafelski editors. Proceedings of an international conference held in Tucson, AZ October 6-12, 1988. Concluding article in section: *Strangeness and Phase Transitions.*

rates in plasma permit us to anticipate near symmetry between u, d, s - quark flavors.

The most critical input needed for a quantitative prediction of strange particle abundances and understanding their source is the nuclear stopping power. In this paper, I briefly survey some theoretical tools, not yet described with sufficient detail during this meeting, which are needed to understand and interpret the results related to nuclear stopping, and indicate how I view different aspects of the experiments, first with respect to the question of nuclear stopping power, and secondly concerning possible new reaction mechanisms in strange particle production.

NUCLEAR MATTER STOPPING AND PARTICLE SPECTRA

I begin with some simple matters which arise mostly from general definitions of the variables and remain true irrespective of the details of the reaction. For the purpose of definition and clarity of notation let me restate in the following a few well-known relations. The appropriate variable, rather than the longitudinal (i.e. along the collision axis) momentum $p_\parallel$, is the rapidity y as it is additive under changes of the frame of reference along this axis. First we recall:

$$\begin{aligned} p_\parallel &= E_\perp \sinh y \ , \\ E &= E_\perp \cosh y \ , \\ E_\perp &= \sqrt{m^2 + p_\perp^2} \ . \end{aligned} \tag{1}$$

For practical reasons, one often refers in an experiment which does not measure the mass of a particle to so-called pseudo-rapidity η.

$$\eta = \ln(\cot\theta/2) \ , \tag{2}$$

where θ is the scattering angle of the emerging particle in the laboratory frame. Rewriting Eq. 2 in terms of momenta we find:

$$\eta = \ln \frac{p + p_\parallel}{p_\perp} \ , \tag{3}$$

which should be compared to the definition of y written in a similar form:

$$y = \ln \frac{E + p_\parallel}{E_\perp} \ . \tag{4}$$

We see that η is asymptotically equal to y in the limit of m being negligible compared to $p_\perp$. This cannot always be true; we know that particles are produced with an exponential $p_\perp$ distribution and hence many will have small $p_\perp$.

Especially in the baryon-rich region, the error inherent in the usage of pseudo-rapidity may be unacceptably large, unless the acceptance of the experiment is limited to large $p_\perp$.

The rapidity particle spectrum dn/dy is derived by recalling that the rapidity in Eq. 1 replaces the longitudinal momentum as a variable. Thus if $f(p_\perp, p_\parallel) = \bar{f}(E; y)$ is the particle spectrum, the rapidity spectrum is simply given by

$$\begin{aligned} \frac{dn(y)}{dy} &= \int d^2p_\perp \frac{dp_\parallel}{dy}|_{p_\perp} \bar{f}(E, y) \ , \\ &= \frac{2\pi}{\cosh^2 y} \int_{m \cosh y}^{\infty} dE E^2 \bar{f}(E, y) \ . \end{aligned} \tag{5}$$

This equation is in the CM-frame; in order to transform it into another (e.g. *lab*) reference frame, y is simply replaced by $(y - y_{cm})$ on the right hand side. Note that if the momentum distribution f were to be spherically symmetric in the CM-frame, $\bar{f}$ would be a function of E only. Hence, for massless particles with *any spherical momentum spectrum* in the CM-frame characterized by the sum of all particle momenta being zero, the $y-$spectrum is of the $1/\cosh^2$ type, which in the laboratory has the appearance of a Gaussian centered at y_{cm}, with a FWHM width of about 1.75 rapidity units. I did not assume here any specific "thermal" form for $\bar{f}$, as has been implied elsewhere. If the dominant scale of energy is the particle mass, the effective range of the integral in Eq. 5 is very limited, and indeed calculations with typical distributions show that the normalized distribution narrows with increasing m, approaching the $\delta-$function form.

In most instances, a particle distribution still wider than the case $m = 0$ in Eq. 5 is observed because the decay of meson resonances further widens the distribution: pions, as the lightest hadronic particles, are often descendants from hadronic resonances. Indeed, assuming thermal relative abundances for a thermal ρ-spectrum at $T \approx 190 MeV$, half of the pions are secondary. Consider for example the decay of the ρ-meson into two pions. Each pion carries energy $E_\pi = m_\rho/2 \equiv \gamma m_\pi$. If by chance the pions are aligned with the $\|$- axis we have a pion of rapidity y_d =1.67, cf. Eq. 4. Averaging over angles, the rapidity distribution of pions originating from ρ decays is found to be

$$\frac{dn^{(2)}(y)}{dy} = \frac{\gamma}{\sqrt{\gamma^2 - 1}} \int_{-y_d}^{+y_d} dy_1 \, \frac{1}{cosh^2 y_1} \frac{dn^{(1)}(y - y_1)}{dy} \ , \tag{6}$$

where $y_d = \ln(\gamma + \sqrt{\gamma^2 - 1})$. The distribution Eq. 6 is normalized to two as there are two pions for each ρ-meson. Calculation shows that, at T=200 MeV, a rather narrow ρ -rapidity distribution leads to a pion distribution with a width of about two units of rapidity.

Uncertainty about the participating masses of the projectile and target nuclei in the common fireball can also be translated into an expression for uncertainty in y. We first determine the central rapidity, that is, the rapidity of the hypothetical system of two colliding objects, such that the net longitudinal momentum of all emerging particles, and hence the longitudinal momentum brought into the reaction by projectile and target, add up to zero. In order to predict the frame of reference in which this is true, we must know the participating mass of the projectile and target. In a symmetric collision of, say, S on S, this is clearly possible, but even in this symmetric case not for each individual collision but only as an average over all collision events. In the case of heavy targets, the number of target nucleons participating in the collision also depends on the impact parameter between the colliding nuclei. Even if all projectile nucleons participate in the reaction, however, the number of target participants can, for heavy targets, still fluctuate strongly, for both geometric and dynamical reasons, since the stopping is probably due to a nonlinear, and hence unpredictably chaotic, response of the medium.

I find that the central rapidity of two colliding masses, as defined above, is:

$$\begin{aligned} y_{cm} &= y_p/2 - 1/2 \ln (M_t/M_p + \frac{E_p - p_p}{M_p}) + 1/2 \ln (1 + \frac{M_t}{E_p + p_p}) \\ &\approx y_p/2 - 1/2 \ln (M_t/M_p) \ . \end{aligned} \tag{7}$$

Here, the lower indices p, t refer respectively to the projectile and target participating in the collision. Using Eq. 7 it follows that

$$\delta y_{cm} = \frac{1}{2}\frac{\delta M_p}{M_p} - \frac{1}{2}\frac{\delta M_t}{M_t} \ . \tag{8}$$

For a "reasonable" range of triggered events, we are selecting a range of M_t, M_p which leads according to Eq. 8 to an uncertainty of y_{cm} which is significant, perhaps as high as 0.3 units of rapidity *in the ensemble of the collision events*.

Thus we see that these two effects (decay and fluctuation of the target mass) can widen the pion rapidity distribution by about 0.5 rapidity units to perhaps a width of 2.3 units, not quite reaching the width of 2.8 units in the rapidity spectrum seen by some experiments. The point is that, as these examples show, such width is not necessarily indicative of nuclear transparency and only detailed modeling which includes the numerous effects contributing to the widening of the distribution will permit one to judge this point. Indeed, I am ready to argue that the observed peaked rapidity distribution signals the unexpectedly nonlinear response of the colliding system and entails unexpectedly large nuclear stopping at CERN energies.

Further qualitative information pertinent to this discussion can be obtained by studying the amount of transverse energy generated in these collisions: the higher the transverse energy, the less memory the system has of the collision axis (transparency). In order to get to the heart of this problem, I need to backtrack to some quite elementary matters. The quark structure of nuclei tells us that it is virtually impossible to find a parton in the nucleus with, say, a fraction $x = 3$ of the total momentum ($x = 1$ is the kinematic limit per nucleon, hence $x = A_p$ is the kinematic limit for the whole nucleus). Consequently, a nucleus has to be treated as consisting of A_p loosely bound nucleons, with internal momentum structure reaching out to perhaps $x \approx 1$ rather than $x = A_p$. This implies that it is inappropriate to treat the projectile and target as monolithic blocks of matter. The proper way to understand the collision kinematics involves the visualization of the collision process as a series of successive collisions: progressive transfer of longitudinal energy to transverse motion reduces the available $\sqrt{s}$ in subsequent collisions. In order to obtain the energy actually available, we must allow for the fact that all particles have a significant motion with respect to the CM-frame which arises in consequence of numerous individual microscopic collisions of the constituents. (These remarks imply that Eq. 7 above is not quite correct. I find an additional shift downward of 0.1 rapidity units, but will not pursue this point here.)

Next, we consider the energy and transverse energy of a fireball in the laboratory frame, assuming that it retains no memory of the collision axis after the collision. This is equivalent to saying that $\bar{f}$ is isotropic in the fireball rest frame and therefore a function of E only. The question is: how large can the transverse energy be; how can different colliding systems be related to each other? We return to Eq. 5. In order to find the rapidity distribution of energy, the energy spectrum of particles in the fireball rest frame $\bar{f}$ must be weighted with the energy of each individual particle i in that frame, $E^i_f = E^i_\perp \cosh y_{i,cm}$, which in the laboratory frame is

$$E^i_{lab} = E^i_\perp \cosh\left(y_{i,cm} + y_{cm}\right) \ , \tag{9}$$

and so the total fireball energy rapidity spectrum in the lab is

$$\begin{aligned} \frac{dE^f_{lab}}{dy} = \frac{d\sum E^i_{lab}}{dy} &= \int d^2p_\perp \frac{dp_\parallel}{dy}|_{p_\perp} E_\perp \cosh(y + y_{cm}) \bar{f}(E) \\ &= 2\pi \frac{\cosh(y + y_{cm})}{\cosh^3 y} \int_{m\cosh y}^{\infty} dE\ E^3 \bar{f}(E) \ . \end{aligned} \tag{10}$$

Integrating over y, only the even component of $\cosh(y + y_{cm})$ survives and so

$$E^f_{lab} = \int_{-\infty}^{+\infty} dy\ \frac{d\sum E^i_{lab}}{dy} = 2\pi \cosh y_{cm} \int_{-\infty}^{+\infty} \frac{dy}{\cosh^2 y} \int_{m\cosh y}^{\infty} dE\ E^3 \bar{f}(E) \ . \tag{11}$$

The coefficient of $\cosh y_{cm}$ can be identified with the observable invariant mass M_f of the fireball created in the collision,

$$E^f_{lab} = \gamma_f M_f = \cosh y_{cm} M_f \ , \tag{12}$$

as the total fireball has zero $p_\perp$. The origin of Eq. 12 is easily explained by noticing that Eq. 1 implies, with $p_\parallel = p\cos\theta$,

$$\frac{dy}{\cosh^2 y} = \frac{p}{E}\sin\theta\; d\theta\ , \tag{13}$$

which immediately permits us to write M_f as

$$M_f = 2\pi \int_0^\pi d\theta\ \sin\theta \int_0^\infty dp\; p^2 E\bar{f}(E) = \int d^3p\; E\bar{f}(E)\ . \tag{14}$$

In other words, the energy content of the fireball in its rest frame is identical to its mass, a formulation consistent with normal relativistic nomenclature.

Finding the rapidity spectrum of the fireball transverse energy is even easier as all transverse energies $E_\perp^i$ and $E_\perp^f$ are Lorentz-invariant. The $\cosh(y+y_{cm})$-term in Eq. 10 simply falls away and we obtain

$$\begin{aligned}\frac{dE_\perp^f}{dy} = \frac{d\sum E_\perp^i}{dy} &= \int d^2p_\perp \frac{dp_\parallel}{dy}|_{p_\perp} E_\perp \bar{f}(E) \\ &= \frac{2\pi}{\cosh^3 y}\int_{m\cosh y}^\infty dE E^3 \bar{f}(E)\ . \end{aligned}\tag{15}$$

If the constituents of the fireball are effectively massless, the transverse energy distribution is therefore of the $1/\cosh^3(y+y_{cm})$-form and the integral over all y can be carried out analytically,

$$E_\perp^f = \sum E_\perp^i = \frac{M_f}{2}\int_{-\infty}^{+\infty}\frac{dy}{\cosh^3 y} = \frac{\pi}{4}M_f\ . \tag{16}$$

Thus in the case of isotropic $\bar{f}$, up to 80% of the fireball's rest system energy may end up in transverse motion. More importantly, Eq. 15 indicates that the distribution of transverse energy can provide additional information about the stopping power, in particular if it is measured as function of rapidity.

This brings us to the question how M_f can be derived from measured rapidity distributions of transverse energy. We proceed as in Eqs. 10 and 15: The total available energy in the laboratory frame is the sum of the projectile energy and that part of the target mass which participates in the collision, M_t:

$$\begin{aligned} E_{lab}^f &= E_{p,lab} + M_t = \sum_i E_{lab}^i = \sum_i E_\perp^i \cosh(y_{i,cm} + y_{cm})\ , \\ &= \cosh y_{cm}\int_{-\infty}^{+\infty} dy\ \cosh y \left(\frac{d\sum E_\perp^i}{dy}\right)\ , \\ &= \frac{E_\perp^f \cosh y_{cm}}{(\pi\Gamma)^{1/2}}\int_{-\infty}^{+\infty} dy\ \cosh y\; e^{-y^2/\Gamma}\ , \end{aligned}\tag{17}$$

where we have assumed for simplicity that the transverse energy distribution has a Gaussian form (rather than the more complex form of Eq. 15):

$$\frac{1}{E_\perp^f}\frac{dE_\perp^f}{dy} = \frac{1}{(\sum E_\perp^i)}\frac{d(\sum E_\perp^i)}{dy} = \frac{1}{(\pi\Gamma)^{1/2}}e^{-y^2/\Gamma}\ . \tag{18}$$

The integral is straightforward and we obtain

$$E^f_{lab} = E^f_\perp \ \cosh y_{cm} \ e^{\Gamma/4} \ , \tag{19}$$

and so, in light of earlier observations,

$$M_f = E^f_\perp \ e^{\Gamma/4} \ . \tag{20}$$

This means that measurement of total transverse energy and the width of the distribution Γ give us a measure of M_f.

Normally, experimental results are presented as a distribution of how often one finds a particular transverse energy within a sample of triggered events. Ideally, this would be a Gaussian function. However, at low transverse energies one sees a significant tail, while the expected structure begins to emerge at high transverse energies, especially for Sulfur-heavy nucleus collisions. This can be due to a distribution in y_{cm} arising from the fluctuation of the number of participating projectile and target nucleons at a given triggering condition. To establish a quantitative relation between the transverse energy and participating masses, I rewrite Eq. 16 in several ways:

$$\begin{aligned}
\ln \sum E^i_\perp &= \ln \frac{\pi\,(M_p \cosh y_p + M_t)}{4\cosh y_{cm}} \ , \\
\ln \sum E^i_\perp &= \ln \frac{\pi}{4} + y_{cm} + \ln M_t \ , \\
\ln \sum E^i_\perp &= \ln \frac{\pi}{4} + \frac{1}{2} y_p + \frac{1}{2}\ln(M_t M_p) \ ,
\end{aligned} \tag{21}$$

where we used the relation Eq. 7. We can therefore write

$$\frac{dN_{event}}{d(\ln \sum E^i_\perp)} = \frac{dN_{event}}{d(\ln \sqrt{M_t M_p})} \ , \tag{22}$$

suggesting that transverse energy distributions should be shown on a logarithmic transverse energy scale. This permits not only to relate the distribution of transverse energy events to the distribution of participating projectile and target masses, but also to relate results obtained with different projectiles and shows how M_t changes with M_p.

Using the approach presented above, I have analyzed some of the data involving 60 and 200 GeV Oxygen and Sulfur collisions with heavy nuclear targets, employing the equation of state of a perturbative QGP with $\alpha_s = 0.6$. I find near-complete stopping in this data. Others may well get different results, since experiments are biased by triggering conditions which sample some particular distribution of events with more or less stopping. However, as strange particles are dominantly made in dense fireballs, particularly in QGP, the best way to proceed is to start with a strangeness trigger, e.g. a kaon, and then to analyze signals such as strange antibaryons for questions related to QGP formation or hyperons for measurement of baryon density.

After the extensive discussion at this meeting of the recent results and the theoretical and experimental surveys there is little space left, if any, for another assessment of the current experimental and theoretical position. But I will permit myself today to take some subjective positions and re-evaluate some results.

Experiment E802 with 14.5 A GeV/c Si-Au collisions at Brookhaven has obtained the transverse energy spectra of charged strange and non-strange particles at various rapidities. Let us first look at the protons in the collision: has the baryon number been stopped? Recall first that, according to Eq. 1, the transverse energy is related to total energy by $1/\cosh y$. Hence, if the particle spectrum is a function of E rather than of $E_\perp$, a cut through an $E_\perp$ spectrum at fixed rapidity will lead to a rapidity- dependent slope parameter, changing according to $\cosh^{-1}(y + y_{cm})$. The slope parameter of transverse momentum distributions of protons as a function of rapidity shows just this behavior, with the central rapidity $y_{cm} = 1.2$ consistent with the Si-tube(Au) kinematics, as noted by E802. This peak is also seen in the peaked charged particle pseudo-rapidity density. These results indicate the presence of a baryon-rich central fireball.

We next look at the strange particle spectra obtained by E802. My past studies lead me to expect that the s-quarks will be mostly bound in baryons, while the $\bar{s}$-quarks will be mostly found in kaons (K^0, K^+), under the assumption that relative chemical equilibrium is established in the dense matter. Hence, assuming that the abundance of pions is charge-symmetric, and using them as a normalizer, it is not surprising to see that K^+ are more abundant than K^-. What is *unexpected* is the result that at $E_\perp > 0.6$GeV the yield of K^+ is equal to the yield of π^+. This is shown in Fig. 1, drafted from the report of the E802 collaboration. In the upper portion the negatives and in the lower portion the positives are shown. The data is preliminary as not all acceptance corrections have been applied: however, the rapidity windows for the respective sets are similar, and hence the ratios mentioned above will very likely remain the same. These results imply in particular similar ability to form $\bar{s}$ and $\bar{d}$ by the nuclear fireball. This is a very significant experimental finding and it would be most interesting to see if it is an accidental coincidence of particle abundances or if it persists for different collision partners at different energies.

Another most striking feature of the data shown in Fig. 1 is the similar structure of the spectra of strange and non-strange mesons, with the slope parameter being about 170 MeV, which points to a thermal mechanism of particle formation. It is most important that the simulations of strangeness production in conventional schemes like Fritiof, when normalized to the pion yield, fail to account for the strangeness abundance by a factor which can be as high as four. On the other hand, the data is compatible with the following

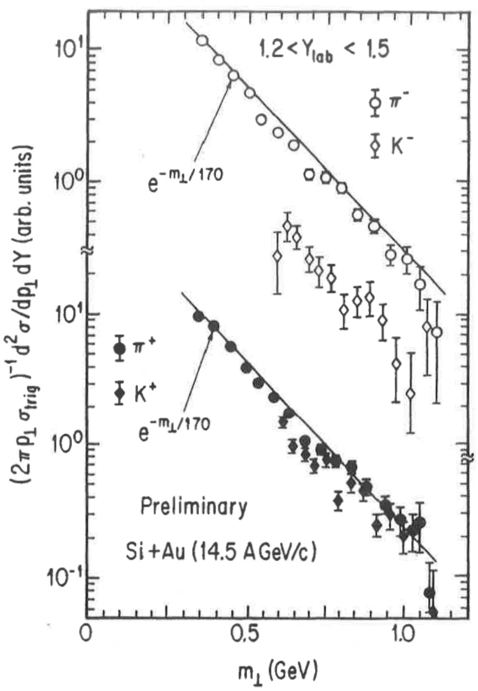

Figure 1: BNL E802 π/K invariant cross sections versus transverse mass (arbitrary units) for Si-Au at 14.5 A GeV/c. Exponential lines drawn by hand (after S. Steadman).

simple QGP model: in T=170 MeV QGP, half of the strangeness phase space can be saturated before the fireball dissociates. Then we know that due to the large baryo-chemical potential the $\bar{s}$ abundance is similar to the $\bar{d}$ abundance, and we can expect that this is reflected in the 'hard' ($E_\perp$ >700 MeV) meson abundances.

Rather large slope parameters are observed for protons (230 MeV) and deuterons (350 MeV) in the same rapidity interval around y =1.2. One should note that the recombination of two thermal nucleons into a deuteron would yield a spectrum with the same thermal slope; only the pre-exponential power describing the density of states in an energy interval changes. This indicates that these hard baryons do not arise from a thermally equilibrated environment. The most obvious explanation is a side splash of quark matter brought into the collision, similar in nature to Greiner's ideas from 15 years ago considered at the time for the nucleons (see his report).

I believe that this experimental evidence is already totally convincing with regard to the behavior of the baryon number and hence conclude that up to E = 14.5 A GeV/c on a heavy target practically total stopping will be found for near-zero impact parameter collisions, with possible collective hydrodynamic three-dimensional baryon (valence quark) flow. The data on strangeness are consistent with the QGP hypothesis. If more data were available at different energies and target-projectile combinations, this reaction mechanism could be ascertained. At present, we only have hard evidence for the formation of nuclear matter of high energy density; any further reaching interpretation of the BNL E802 data is premature.

Complementary data on strange particle production in highly excited nuclear matter has been shown in the KEK results of 3 and 4 GeV/c $\bar{p}$ annihilation on Ta: a strongly peaked, anomalously large thermal distribution of Lambdas around the laboratory rapidity 0.25 has been found. In Fig. 2 the results presented by Miyano (KEK) are shown: in order to emphasize the difference to the $\bar{p}p$ reactions the data in this figure is presented shifted to the rapidity of the elementary reaction on individual nucleons. We see that the strong shift in the rapidity distribution and central rapidity is that of a reaction with a matter tube in the target in front of the projectile. The shape displayed by the distributions corresponds closely to the thermal rapidity spectrum of about 100 MeV. I presented a detailed discussion of these results in terms of QGP elsewhere and I will not repeat the arguments again, except to mention that, were it not for the relatively large $\bar{\Lambda}$ abundance seen, I could agree with the suggestion of C. Dover and P. Koch (see their report, also for references) that these results are also obtainable with a model of a dense hadronic gas. Again, a more complete analysis will only distinguish between these two competing reaction channels, and this requires much more data, both as a function of $\bar{p}$ energy and the size of the target. As with the BNL E802 data, one “point” in the parameter space can always be fitted by several models. We need the systematic behavior of these global observables in order to be able to argue the case for the different hadronic phases.

What about CERN experiments at 60 and 200 A GeV with Oxygen and Sulfur projectiles? Today everybody seems to agree that there is still a large amount of stopping, in particular in collisions involving heavy nuclei: The baryon number is not shooting out of the central rapidity region, nor have the hadronic fireballs separated into projectile and target fragmentation regions. We are also continuing to see large transverse momenta.

Consider the rapidity distribution of particles: the NA35 report shows little difference between the rapidity distribution of negatives produced in symmetric S-S collisions and p-p collisions at the same energy per nucleon. This could be taken to indicate that little difference, if any, is encountered in these collisions, whatever the underlying reaction mechanism. Earlier data from NA35, however, showed a strongly peaked rapidity distribution of negative particles in collisions on heavy targets, and we have seen in the report of M. Tincknell a highly peaked transverse energy distribution, as a function of rapidity. Other evidence for a geometric and hence totally inelastic reaction comes from the $A_t^{2/3}$ behavior of the transverse energy. In all cases, the position of the multiplicity and transverse energy peak is as expected for complete

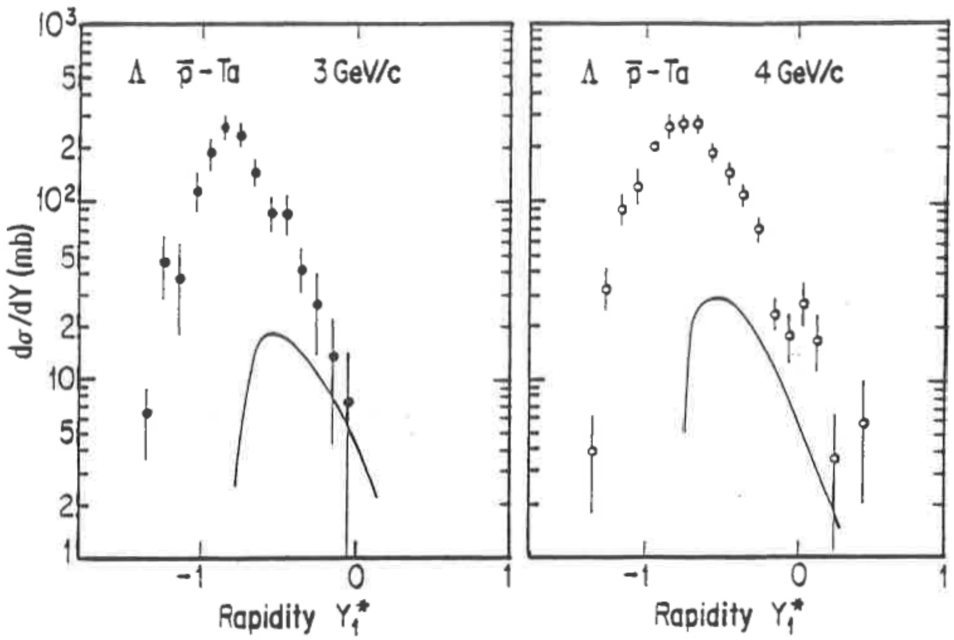

Figure 2: KEK rapidity spectrum of Λ in $\bar{p}-$Ta annihilations at 3 and 4 GeV/c. Solid curves are $A^{2/3}$ scaled $\bar{p}p$ spectra. Rapidity 0 corresponds to the colliding $\bar{p}p$ system (after K. Miyano).

stopping of the projectile by the participating target matter, and the width of the distribution is compatible with our discussion presented above.

Maybe the conclusion to be drawn is not to pursue S-S collisions, as the chance of a punch-through is too great; perhaps we should concentrate our effort on heaviest targets, as there is a greater chance to stop the projectile within the 15 fm diameter of the target nucleus. This point is further supported by the observations of P. Stevenson about the geometric nature of the p-Nucleus interaction. Both these points, excess of u,d quarks in the central region as well as the sharp edge geometry of the collision, do not preclude "transparency", in particular in the sense that different reaction mechanisms are of importance. A quantitative estimate is needed about the relative frequency of the various reactions. A step in this direction was undertaken; however, the reported initial positions stated in the report of P. Braun-Munzinger differ from our above observations about the experimental results to such a degree that we cannot take the analysis presented there as being conclusive. The experimental data must first be consistent with the assumptions of this analysis.

We have seen several specific presentations of the CERN data addressing the question: is there any signature of QGP in the current strange particle results? The reports of M. Gazdzicki and I. Derado (NA35 collaboration), see Figs. 3 and 4, have focused on the absolute Λ abundance, the report of E. Quercigh (WA85 collaboration) has shown first results on strange antibaryons, and in particular the relative strength of $\bar{\Lambda}/\Lambda$ were presented as a function of

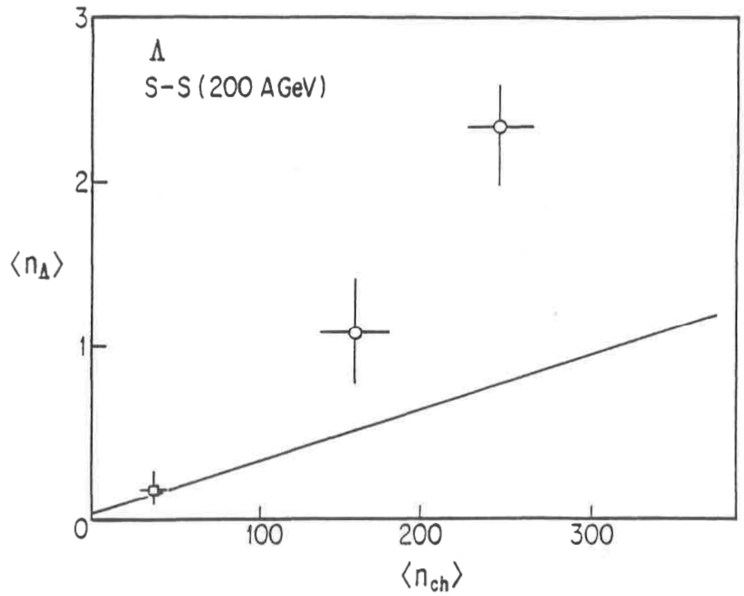

Figure 3: NA35 Λ versus charged particle multiplicity in S-S collisions at 200 A GeV. Solid line: superposition yield of nucleon-nucleon collisions (after M. Gazdzicki).

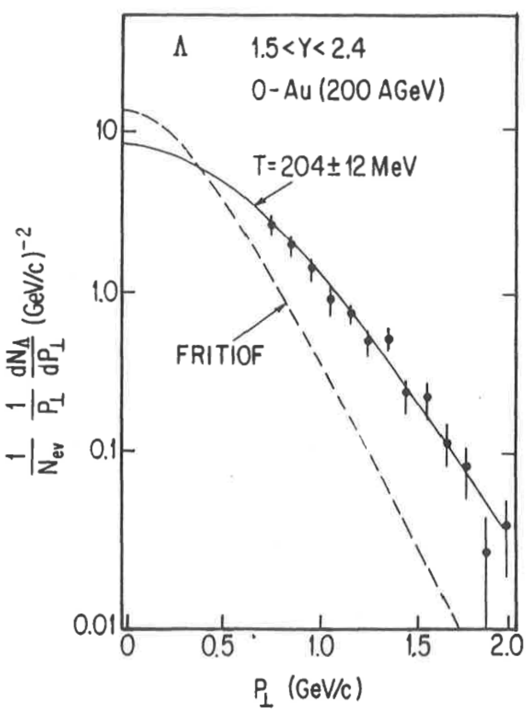

Figure 4: NA35 Λ transverse momentum spectra from O-Au 200 A GeV collisions. Solid line: Fritiof simulation (after I. Derado).

the transverse momentum in the central rapidity region, see Fig. 5. The first rapidity distribution of Λ of NA36 was shown by D. Greiner.

In my view, the main interpretation arising from these reports is: there is a clear signal of something unusual happening; there is more strangeness than expected from particle cascades or other conventional simulations, most boldly pointed out in the report of M. Gazdzicki (see Fig. 3), and there are more $\bar{\Lambda}$'s than one would normally anticipate in the WA85 data, even taking the optimistic view that the $\bar{p}/p$ ratio from p reactions is a guide to the expected abundance. This enhancement of $\bar{\Lambda}/\Lambda$ seems to depend little on the multiplicity of charged particles observed in coincidence. But there may be some transverse momentum dependence, as shown in Fig. 5. In a QGP approach, the high momenta are populated early on, and the decrease in the ratio may signal a greater baryon density in the early stages of the fireball, favoring Λ production and inhibiting light anti-quarks needed. In order to verify these observations, one would need to consider multi-strange baryons and antibaryons, which should show a flat or even increasing ratio as a function of the transverse momentum. It is interesting to observe that the Λ enhancement at high $\mathrm{p}_\perp$ is also very clearly present in the data of I. Derado, c.f. Fig. 4. Although he is disclaiming it in his paper, his results show enhancement of the yield in the central rapidity region for O-Au reactions, by one order of magnitude for $p_\perp > 1.5\mathrm{GeV/c}$. The most notable point of the NA36 data is the concentration of the yield in the central rapidity region. Clearly, many of these results are preliminary and therefore theoretical implications should not be taken too far right now.

While the presented results on strange particle abundances agree almost exactly with earlier predictions about the QGP response, we have presently only one point in the parameter space, and it is conceivable that an alternative interpretation of the data may be found; however, a price will be paid in terms of other observables which may turn out to be inconsistent with the general reaction picture. For example, recent work which attempted to produce a lot of strangeness in hadronic gas needed to employ high temperature to overcome the Kaon production threshold. However, there is no sign in particle spectra of temperatures as high as 350 MeV, not to mention the internal inconsistency of an approach in which higher meson and baryon resonances are neglected to reduce the specific heat of the hadronic gas. Secondly, efforts to dilute the strangeness signal of QGP by producing many pions via soft processes have to be contrasted with entropy balancing: if the pions are produced after the QGP phase, then the initial entropy in the plasma was much less than currently believed, implying a much lower temperature in the plasma than qualitatively acceptable. We see again an internal inconsistency of the approach. It is therefore very tempting to conclude that indeed we are on the right track toward discovery of the QGP, and that strangeness is a suitable signature of new phenomena arising in highly excited and compressed nuclear matter.

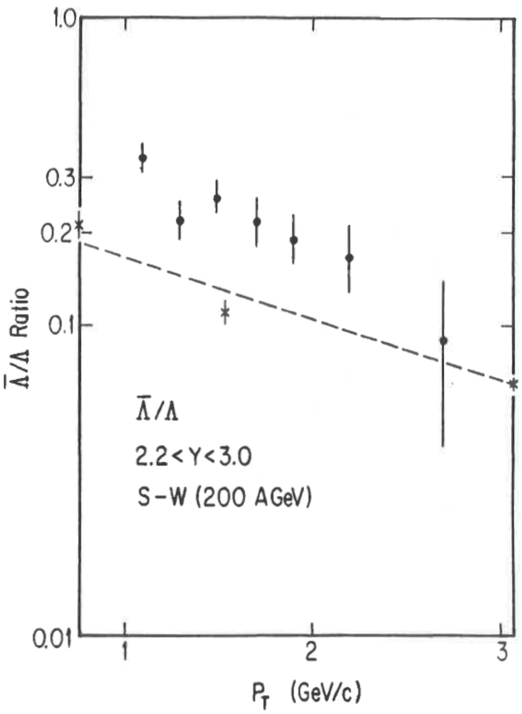

Figure 5: WA85 $\bar{\Lambda}/\Lambda$ versus $p_\perp$ for S-W at 200 A GeV, compared to p-W at 200 GeV $\bar{p}/p$ ratio at x=0 (after E. Quercigh).

Acknowledgment: Many insights presented here were obtained in collaborative efforts. I want to give particular credit to: R. Hagedorn, for teaching me statistical particle production models; B. Müller, for collegial and remarkable collaboration over many years and P. Koch, for his willingness to venture into the unknown. References to other papers in these proceedings are self-evident. This work was in part supported by the US Department of Energy, AEP division.